6 Structural Studies of Prion Proteins

Stephan Schwarzinger, Dieter Willbold, and Jan Ziegler

6.1 Introduction

The previous chapter dealt with the biophysical characterization of recombinant mouse prion protein. This included a first characterization of the conformation of the cellular form of prion protein (PrP^C) by circular dichroism (CD) spectroscopy, which indicates a significant amount of helical structure in the cellular isoform. CD has also been successfully applied to study conformational changes, for example, introduced by the addition of small amounts of the denaturant sodium-dodecylsulfate (SDS) resulting in changes of the oligomeric state as well as the secondary structure content depending on the amount of SDS (see Chapter 8). However, techniques such as CD do not allow precise localization of where certain secondary structure elements are positioned or are involved in structural changes. Ultimately, for the understanding of basic principles underlying the conversion of PrP^C into its scrapie isoform (PrP^{Sc}), knowledge of both conformations and eventually of intermediate conformations at atomic detail is required. The situation is shown schematically in Figure 6.1. In this chapter we review the current state of high-resolution structural studies on prion proteins. Besides the wealth of experimental data, which are available at present on the structure of the globular part of PrP, we will outline new approaches on fragments of PrP, interacting ligands, hydrogen exchange and insoluble, PrP^{Sc}-like conformations or PrP, where we can expect further progress in the future.

At present there are only two methods available that provide true resolution at atomic detail, namely, nuclear magnetic resonance (NMR) spectroscopy and X-ray crystal diffraction. In the following we shall briefly review the principles underlying these two techniques. X-ray crystallography utilizes the fact that an electromagnetic beam is scattered by the electron clouds in a single crystal of a given compound. In a single-crystal, molecules are arranged into a so-called asymmetric unit, which is periodically repeated in the three directions of space. If the crystal is hit by an X-ray beam the asymmetric unit produces a particular pattern of scattered rays, typical for the space group in

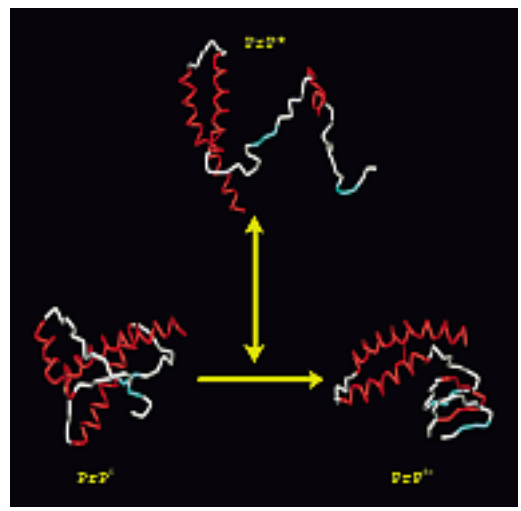

Fig. 6.1: Schematic representation of the conformational changes related to the conversion of cellular prion protein (PrP^C) into the pathogenic form (PrP^{Sc}). Knowledge of the conformations of PrP^C, PrP^{Sc}, and intermediate states called PrP^{-} will provide important insights into the infectious mechanism of transconformation. The structure of PrP^C has been experimentally determined by NMR [Protein Data Bank (PDB) code 1QM2]. PrP^{Sc} has been modeled as described [64], and the schematic PrP* has been obtained from a molecular dynamics (MD) unfolding simulation. ©: Figure by S. Schwarzinger with WebLabViewer Lite, Accelrys, San Diego.

which the crystal grew. Structural information is extracted from the phases and intensities of the individual spots from patterns obtained from numerous different orientations of the crystal in the X-ray beam. The caveats of this technique are that (i) a protein crystal of suitable size and quality has to be grown, and (ii) that the phases of the signals are a priori unknown. Crystallization usually requires screening of large numbers of crystallization conditions, and today is often achieved by utilizing crystallization robots. Phases are routinely obtained by isomorphous heavy-metal replacement, molecular replacement, or more recently, by multiwavelength anomalous diffraction (MAD) techniques. Protein crystallography usually yields positions of the heavy atoms of a protein and can be applied to rather large molecular assemblies, such as the proteasome. However, crystallography of proteins with rather large flexible parts is problematic, either because no crystals can be grown at all or because of large conformational flexibility in the crystal, prohibiting recording of suitable reflections from the flexible parts.

In contrast, high resolution NMR spectroscopy traditionally works in aqueous solutions. It makes use of the radio frequency response that is obtained when a magnetically active nucleus is put into a strong external magnetic field and perturbed by a radio frequency pulse. The radio frequency obtained depends on the local magnetic field of a nucleus, which in turn depends on its chemical environment. Usually, each nucleus can be assigned to a particular resonance frequency. Modern NMR spectroscopy makes use of the magnetically active, stable isotopes ^{1}H (99 % natural abundance), ^{13}C, and ^{15}N, the latter two of which can be conveniently incorporated into the protein via bacterial expression systems. This way in combination with ultra-high field magnets it is now possible to routinely assign the NMR resonances to their respective nuclei and resolve the three-dimensional structures of proteins of up to approximately 25 kDa. This size limit has long been a major obstacle of solution NMR, which, however, has recently been overcome by the development of the so-called TROSY technique. The TROSY technique allows structural studies of proteins and protein complexes of hundreds of kDa [1]. NMR structures have typically been calculated from pairwise interproton distances, available from nuclear Overhauser-type experiments, and torsion angles extracted from scalar coupling constants [2]. Nuclear Overhauser effects (NOEs) can be observed between protons belonging to amino acid residues that may be close or distant to each other within the protein sequence. Observation of such NOEs for a given proton pair indicates them to be close together in space, ultimately yielding an experimentally observed pairwise interproton distance. In general, thousands of these pairwise interproton distances are required to define a high-resolution 3D protein structure. More recently, residual dipolar coupling constants resulting from partial alignment of the protein relative to the external magnetic field have become available as additional structural parameters, which allow the determination of bond vector orientations in space. For example, the relative orientations of amide bond vectors relative to each other are often used as experimental constraints in protein 3D structure determination. In contrast to protein crystallography, solution NMR typically yields an ensemble of converging structures, which already include to some extent information about dynamics within the protein. Typically, these structures are essentially identical for the core and for well-folded parts of the proteins. However, they display structural variation in segments with increased chain flexibility providing information about the extent of motion and alternative conformations or structural disorder in the respective part of the protein. A particular strength of solution NMR spectroscopy is the capability to deal with entirely disordered polypeptide segments, which is of special interest in the context of the intrinsically disordered N-terminus of the PrP, and to extract information about residual or preferred structures in such sequences, for example, from chemical shift deviations [3]. As the only experimental technique available, NMR spectroscopy allows monitoring of internal motions in a molecule on a timescale ranging from nanoseconds to hours. Such studies often reveal

important dynamical and conformational features of both folded and disordered polypeptide chains. Solution NMR has also gained importance when it comes to screening for ligands binding to a particular protein and for mapping binding interfaces, for example, in complexes of biological macromolecules.

Both methods have a common disadvantage, namely that they require extremely pure protein with solubility in the mg/ml range (i. e., high μM to mM concentrations). Therefore, production of substantial amounts of properly folded, soluble PrP is of crucial importance for structural studies. As explained in the previous chapter, PrPs are highly conserved among mammals. PrP^C is translated as a 253-residue protein with a 22-amino-acid N-terminal leader sequence that is cleaved off during transport to the cell surface. There, the protein is attached to the membrane via a C-terminally linked glycolphosphatidylinositol (GPI) anchor. The protein consists of two domains, the N-terminal (residues 23–120) of which is intrinsically disordered. This domain contains an octarepeat segment (51–91, five times PQGG[T/G/S]WGQ) and is capable of binding copper ions [4]. The C-terminal domain (residues 121–231) adopts a predominantly helical globular fold. It contains a disulfide bridge (Cys179 and Cys214), two sites for N-glycosylation (Asn181 and Asn197), and the GPI anchor is attached to Ser231. Initial attempts to express the PrP were hampered by protease activity cleaving the protein preferentially at residues 112, 118, and 120. Therefore, the first expression system that yielded protein in amounts suitable for structural studies included only the globular C-terminal domain, i. e., residues 121–231 [5]. However, highly efficient transcription systems enabled expression of longer, protease-sensitive constructs as insoluble inclusion bodies, which are insensitive to proteolysis and which could be resolubilized and properly refolded. This way it was possible to produce large quantities of full-length PrP (23–231), a PrP fragment lacking the N-terminal part and the octarepeat region (90–231), as well as the fragments solely consisting of the globular domain 121–231 [6; 7]. In the following, we will initially focus on the structural properties of the globular domain of the PrP, the comparison of structures from different species as well as structures from variants that are associated with increased pathogenic potential, before we briefly review studies on protein dynamics, studies of isolated structural features, investigations on molecules binding to PrP^C, intermediate structures, solid state NMR studies, as well as first structural investigations of a scrapie conformer of PrP.

6.2 Structure of the globular domain of PrP^C

The first prion structure made available was the C-terminal fragment of mouse prion protein (moPrP), which was solved by NMR spectroscopy at the Eidgenössische Technische Hochschule in Zurich, Switzerland, in 1996 [8]. A little later, the structure of the fragment 90–231 of Syrian hamster prion (shPrP) was solved by NMR at the University of California, San Francisco [9]. As expected from CD data, both structures displayed a high content of α-helices. As seen in Figure 6.2, the globular domain consists of three α-helices, helix 1 (residues 144–154), helix 2 (residues 175–193), and helix 3 (residues 200–219) with a helix-like extension from resi-

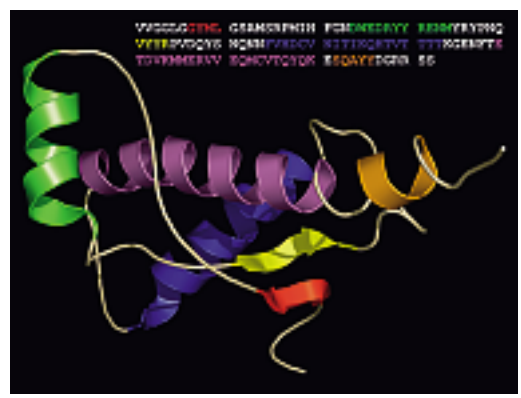

Fig. 6.2: NMR structure of the globular domain of recombinant mouse prion protein (PDB code 1AG2). Elements of regular secondary structure and their corresponding part in the sequence are color coded: strand 1, red; helix 1, green; strand 2, yellow; helix 2, blue; helix 3, magenta; helix 3″, orange. ©: Figure by S. Schwarzinger with PyMOL, DeLano Scientific, San Francisco.

due 222 to 226, as well as a short antiparallel β-sheet with strand 1 extending from residue 128 to 131 and strand 2 from residue 161 to 164. The ensemble of NMR structures converges very well for these elements of regular secondary structure indicating a stable fold. Helices 2 and 3, which do not have a high intrinsic propensity to form helices, are linked and thus stabilized by the disulfide bond. However, increased structural diversity indicating a certain degree of disorder is found in the terminal regions of the polypeptide chain (residues 121–125 and 220–231), but increased backbone flexibility is also detected for the loop between strand 2 and helix 2 (residues 166–171). The N-glycosylation sites are located on the solvent-exposed side of helix 2 and in the loop region between helices 2 and 3.

A central question when analyzing structures of post-translationally modified mammalian proteins that have been obtained by heterologous expression in bacterial expression systems is, whether or not the modifications have a significant impact on the structure. In case of the PrP, which carries a GPI anchor as well as two N-glycan moieties, it was shown that the one-dimensional proton NMR spectra of recombinant bovine PrP and of PrP extracted from calf brains are essentially identical in their most important structural features [10]. Initially, structures have been determined at slightly acidic pH values. Studies of PrP^C at neutral pH, however, revealed an essentially identical structure over the pH range from 4.5 to 7.0. The most pronounced change is a C-terminal extension of helix 1 by about one turn; 3_{10}-helix from residues 153 to 156 as depicted in Figure 6.3 [11]. By comparison of the PrP structure with structures of proteins with known functions [12], a possible signal-peptidase function was predicted as one of several suggestions for the physiological function of PrP^C (see Chapter 7).

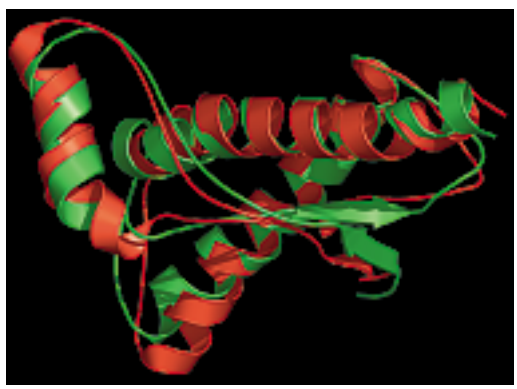

Fig. 6.3: Effect of pH on the structure of human PrP, huPrP(121–231). The NMR structures obtained at pH 4.5 (PDB code 1QM2, shown in green) and pH 7.0 (1HJM, shown in red), respectively, have been overlaid by root-mean-square deviation (RMSD) fitting. The most pronounced changes are observed for helix 1, which is extended at its C-terminus by a turn of a 3_{10}-helix. This causes displacement of the entire helix 1 and the C-terminus of helix 2, which is in contact with helix 1. ©: Figure by S. Schwarzinger with PyMOL, DeLano Scientific, San Francisco.

Based on the known PrP structure, it is possible to locate the amino acid sequence positions for pathogenic mutations and map binding interfaces of other proteins interacting with the PrP. The binding site of the so-called protein X, which is thought to be involved in the pathogenic conformational change to PrP^{Sc} *in vivo*, could be mapped by biochemical experiments to residues 168, 172, 215, and 219 of the human prion protein, huPrP [13]. From the three-dimensional structure, it is clear that these residues are located in close spatial proximity (Fig. 6.4). Also, the binding epitope of the antibody 6H4, which is capable of preventing scrapie formation, was found to coincide almost exactly with helix 1 [14]. Helix 1 itself is remarkable, since it is the most polar helix in the entire structure database. It shares only very few tertiary contacts with the remainder of the protein. Studies on peptide segments yielded a very high tendency to form stable α-helices [15], also discussed in Section 6.4.

Structure determination of PrPs from different species might provide insights into susceptibility for interspecies prion transmission and into the nature of the species barrier. Thus, structures of the PrPs of mouse [8], hamster [9], humans [16], cattle [17], cat, dog, pig, sheep [18], elk [19], chicken, frog, and turtle [20] have been studied by NMR spectroscopy. The structures of sheep PrP [21] as well as huPrP [22] have also been determined by X-ray crystallography.

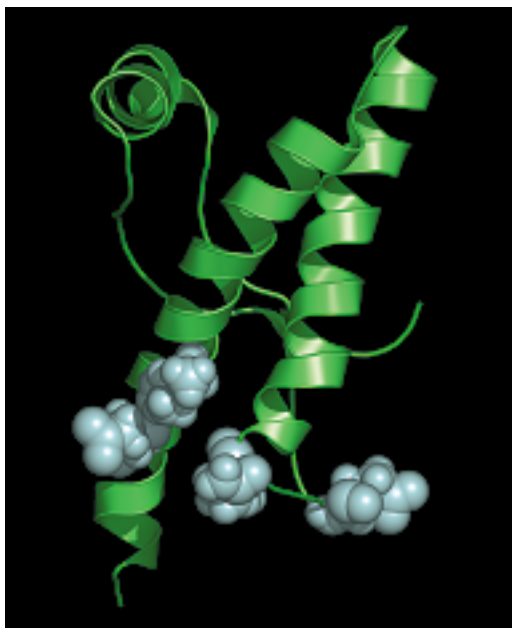

Fig. 6.4: Location of the putative binding interface of "protein X". Residues 168, 172, 215, and 219, shown as cyan spacefill models, represent the proposed binding interface for protein X. ©: Figure by S. Schwarzinger with PyMOL, DeLano Scientific, San Francisco.

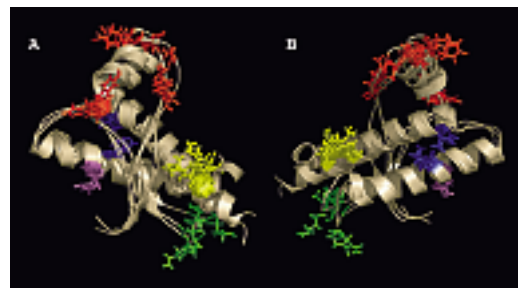

Fig. 6.5: Differences between the structures of the PrP of mouse (PDB code 1AG2), man (PDB code 1QM2), and cattle (PDB code 1DWY). Although the overall fold is well conserved, local differences arise between structures. Positions with differences in the sequence between the three species are colored. A cluster of variations in the sequence is located near or within helix 1 (red), and another cluster is located in the loop between strand 2 and helix 2 (green). Clusters are also found at the C-terminus of helix 3 (yellow) and at the interface between helices 2 and 3 (blue). Another position with differences in the sequence is positioned in the center of helix 2. Figures **(a)** and **(b)** are rotated by 180° for better visibility. Interestingly, the structure similarity between cattle and man is higher that for mouse PrP. ©: Figure by S. Schwarzinger with PyMOL, DeLano Scientific, San Francisco.

In essence, all PrPs studied so far share the same fold. An exception is represented by an X-ray structure of a domain-swap dimer of the huPrP, which will be discussed in more detail below.

An overlay of the structures of PrP^C from mouse, cattle, and man along with differences in sequence is depicted in Figure 6.5. Despite only few differences in sequence and the same overall fold, some deviations in the structures can be seen. In particular, differences in the alignment of helix 1 with the other helices are evident, as well as differences in the orientation of the carboxy-terminus of helix 3. It can also be seen that the structures of bovine and $huPrP^C$ are structurally more closely related than they are to the structure of mouse PrP^C. This actually may indicate why BSE can be transmitted to humans. The recent report on five additional structures of mammalian PrP provides further insights into the possible role of certain structural elements in prion diseases [18]. In particular, it appears that amino acid substitutions in the structurally flexible loop region linking strand 2 and helix 2, which has also previously been assigned as part of the putative protein X binding interface [13], may play an important role in susceptibility to prion diseases. Especially amino acid substitutions which alter charges in this region have been shown to have pronounced effects. For example, sheep carrying the positively charged arginine residue at position 168 of PrP are highly resistant to TSE, while sheep with glutamine or histidine residues at this position display high to medium-high susceptibility for scrapie infection. Based on a comparison of residues varying among different species, the important role of surface charge distribution on the species barrier has already been previously suggested [23].

Amino acid substitutions in the strand 2–helix 2 loop region are reported to have a strong effect on backbone flexibility. Exchange of

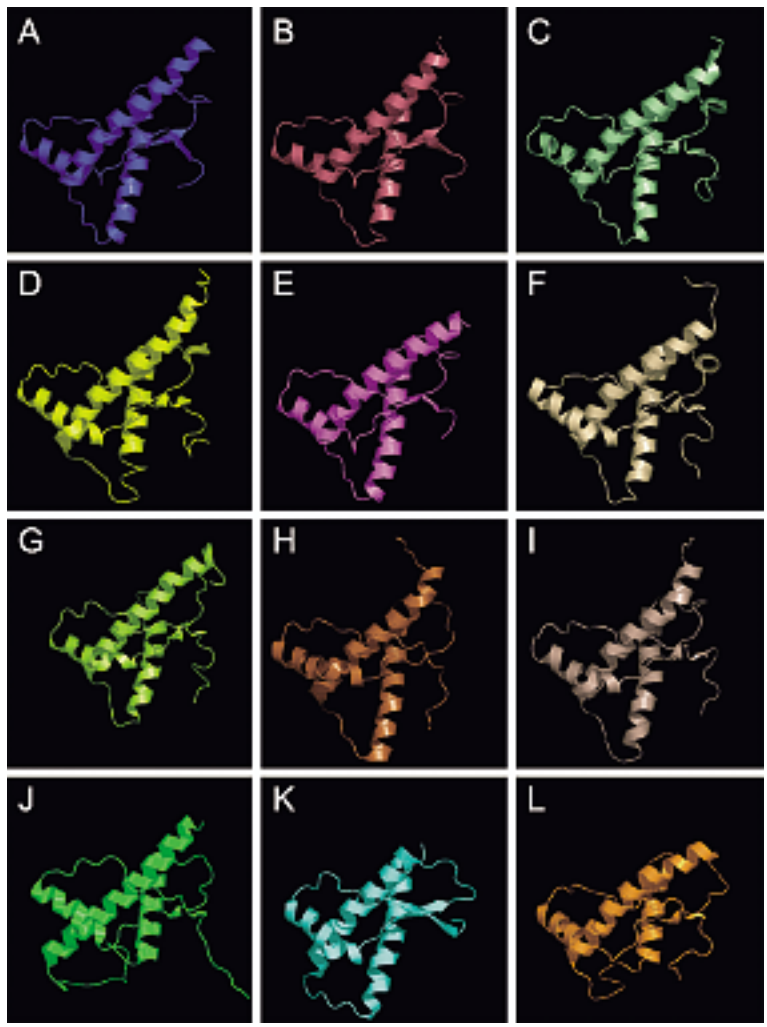

Fig. 6.6: Schematic representation of known PrP structures. The panel shows the structures of the PrP of **(a)** man (PDB code 1QLZ), **(b)** cattle (PDB code 1DWZ), **(c)** sheep (PDB code 1Y2S), **(d)** mouse (PDB code 1XYX), **(e)** Syrian hamster (PDB code 1B10), **(f)** elk (PDB code 1XYW), **(g)** cat (PDB code 1XYJ), **(h)** dog (PDB code 1XYK), **(i)** pig (PDB code 1XYQ), **(j)** chicken (PDB code 1U3M), **(k)** frog *Xenopus laevis* (PDB code 1XU0), and **(l)** turtle *Trachemys scripta* (PDB code 1U5L). While the global fold is well conserved, differences can be found especially in the loop parts and in the positioning of helix 1 relative to helices 2 and 3. In some cases (chicken and turtle), an additional short 3_{10} helix is formed within the globular domain. Despite the low sequence identity of about 30 %, even in these cases the global fold is nearly identical to mammalian prions. Sequence variation within mammalian PrP tends to cluster within the loop 166–172 and at the carboxyterminus of helix 3. Apart from small local structural deviation, these sequence differences do not lead to major structural consequences. However, as these regions are mostly surface exposed, they alter the charge distribution on possible interaction sites of the protein. ©: Figure by J. Ziegler with PyMOL, DeLano Scientific, San Francisco.

Fig. 6.7: Location of disease-related mutations in the PrP structure. Mutations are mapped on the NMR structure of huPrP(121–231) and have been color coded. Residues shown in red are associated with CJD, those shown in green have been found with GSS. Residue Asp178 is found in either CJD or GSS, depending on whether residue 129 is methionine or valine (both residues shown in blue). Thr183 (magenta) is linked to dementia when changed. Mutation of Tyr145 (yellow) into a stop codon also causes disease. Mutations Pro102Leu, Pro105Leu, Ala117Val, and Met232Arg lie outside the globular domain of PrP and are therefore not shown. ©: Figure by S. Schwarzinger with PyMOL, DeLano Scientific, San Francisco.

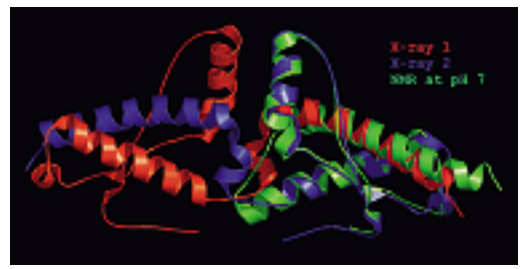

Fig. 6.8: X-ray structure of the domain-swap dimer of huPrP(121–231) (pdb code 1I4M). The dimer is created by rotation along the helix 2–helix 3 loop, so that helix 2 of either monomer (colored red and blue) contacts helix 3 of the other one, and vice versa. The subdomain formed by the β-sheet essentially keeps its orientation relative to the (now domain-swapped) helices 2 and 3. Interestingly, excellent conservation of the native prion fold is revealed when overlaid with the structure of huPrP at pH 7. Structural deviations are most pronounced at the C-terminus of helix 2 and its connecting loop with helix 3. A minor deviation is also observed for the orientation of the C-terminus of helix 3. ©: Figure by S. Schwarzinger with PyMOL, DeLano Scientific, San Francisco.

Asn173 to Ser in pig significantly reduces the structural variability in this region. Similarly in elk PrP^C, this part of the PrP is very stable [19]. Based on studies of mouse/elk hybrid PrPs, it has been shown that residues Asn170 and Thr174 are decisive for introducing rigidity in the strand 2–helix 2 loop.

Recent studies of non-mammalian PrP with a sequence identity of approximately 30% to mammalian PrP [29] revealed that the architecture of PrP is obviously well conserved over large parts of the animal kingdom. However, significant perturbations in local structure were observed (Fig. 6.6).

Another interesting feature of PrP^C structure is that most PrP mutations related to TSE pathogenesis can be found buried in the interior of the protein, while only a relatively small number of affected residues are surface exposed (Fig. 6.7). However, the effect of such mutations cannot be explained exclusively by a destabilization of the globular domain of PrP^C [24].

An X-ray crystallographic study of the huPrP revealed a domain-swapped dimer of PrP [22]. The two monomers orient such that helix 3 of one monomer interacts in a native-like manner with the second monomer forming native-like, although intermolecular disulfide bonds (Fig. 6.8). Formation of the dimer implies opening of the monomeric fold of PrP^C and involves a rearrangement of the native intramolecular disulfide bond. Interestingly, the interface between both monomers contains many "pathogenic" mutations. Thus, it may be speculated, whether a structural rearrangement as observed in the reported dimer plays a role in the conversion of PrP^C to PrP^{Sc}. Up to now, however, a physiological role of a dimer with intermolecular disulfide bonds has not been shown.

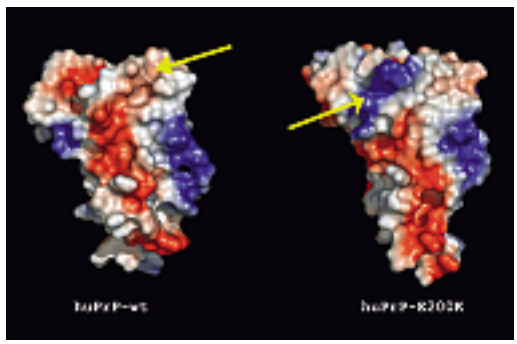

Fig. 6.9: Effect of the "pathogenic" mutation Glu200Lys on the surface charge distribution of PrP. Wild-type huPrP (PDB code 1QM2) and huPrPGlu200Lys (PDB code 1FO7) have been aligned and their vacuum electrostatics have been estimated with PyMOL. Residue 200 is located at the N-terminal part of helix 3. The mutation Glu200Lys leads to a drastic change in the surface charge around this position (marked by arrows). ©: Figure by S. Schwarzinger with PyMOL, DeLano Scientific, San Francisco.

A comparison of the structures of the disease-related mutants Glu200Lys [25] and Met129Val [26] revealed no significant differences. This polymorphism is associated with cases of new variant Creutzfeldt–Jakob disease (vCJD), where patients were shown to be homozygous for methionine at position 129. Furthermore, the mutation Asp178 to Asn is associated with fatal familial insomnia (FFI) when residue 129 is methionine, and with CJD when residue 129 is valine. No differences in structure, dynamics, or stability could be detected between mutant and wild-type protein. This suggests that Met129Val does not act via changes in the structure of PrP^C rather than on the folding or conversion intermediates.

The mutation Glu200Lys involved in familial CJD, is located in the loop connecting helices 2 and 3 at the N-terminus of helix 2. Interestingly, again no structural deviations could be observed between mutant and wild-type protein. The mutation alters the charge distribution at the proteins surface, indicating that surface charge distribution plays an important role in prion diseases (Fig. 6.9).

6.3 Structural studies of full-length PrP

Structural investigations of the flexible N-terminal tail are particularly difficult, as rapid conformational averaging prevents crystallization as well as calculation of structural ensembles from NMR studies. Thus, NMR studies of the structure of full-length PrP only resulted in three-dimensional structures for the globular domain of the protein studies, which are essentially identical to the structures obtained from the isolated C-terminal domains as shown in Fig. 6.10 [16; 17; 27; 28]. However, measurable differences in the structure of the globular domain of huPrP could be detected for the carboxy-terminal parts of helices 2 (187–193) and 3 (219–226). Because these structural variations do not depend on the concentration of the protein over a range from 0.1 mM to 1 mM it was concluded that these structural variations arise from transient contacts to the flexible N-terminus [16; 29].

NMR can reveal differences in the dynamics of individual residues. Measurements of the heteronuclear ^1H-^{15}N Overhauser effect (hetNOE) and of the longitudinal (R_1) and transverse (R_2)

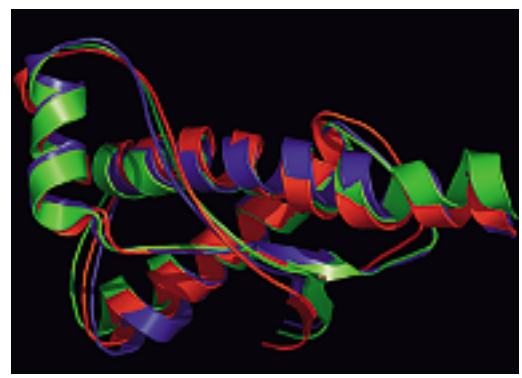

Fig. 6.10: Effect of absence or presence of PrP N-terminal parts on the structure of the globular domain. HuPrP(23–231) blue, PDB code 1QLX; huPrP(90–231) red, PDB code 1QM0; and huPrP(121–231) green, PDB code 1QM2, have been aligned by RMSD minimization. Small structural variations, caused by transient contacts of the flexible N-terminal tail with the globular domain, are centered at the C-terminus of helices 2 and 3. ©: Figure by S. Schwarzinger with PyMOL, DeLano Scientific, San Francisco.

relaxation rates of the amide nitrogen nuclei revealed that the most rigid part of the globular domain is the interface between helices 2 and 3 near the interhelical disulfide bond [30]. Parts of the protein that are not in contact with this core exhibit higher backbone flexibility. Helix 1, which has only a few tertiary contacts with helices 2 and 3, shows increased backbone dynamics in comparison to the core. These data are in line with the structural convergence observed in the NMR-ensembles as well as with amide-hydrogen protection factors (see Section 6.4.3). Methionine 131 in β-strand 1 of sheep PrP undergoes complex motions on the μs to ms timescale that are typical for conformational exchange [30]. Such dynamic behavior in the β-sheet of PrP could be of importance for prion aggregation.

Relaxation measurements have confirmed that the N-terminal region (residues 23–125) does not adopt a compact and stably folded structure. Instead, it samples a large conformational space with a high frequency [30]. Nevertheless, this does not mean that this part of the polypeptide chain moves randomly and does not have residual or preferred structure elements. As previously mentioned, the N-terminal domain appears to be in transient contact with the globular domain [29]. Moreover, the N-terminal domain contains the copper-binding octarepeat unit as well as a copper-binding site involving residues His96 and His111 [31]. Copper, being a paramagnetic nucleus, has so far prohibited high-resolution NMR structures of the copper loaded N-terminus. However, studies of isolated fragments of the octarepeat region reveal presence of a well-defined structure depending on the pH value [32]. Dynamic data derived from hetNOE studies at pH 4.5 and pH 6.2 support this finding by indicating loss of backbone mobility in the central part of the octarepeat region upon pH increase [32]. Similarly, a well-ordered structure could be obtained from NMR studies of octarepeat peptides in micellar environments [33]. It could also be shown that the octarepeat region represents a pH-dependent oligomerization site. Copper binding may modulate this aggregation [32]. For instance, binding of copper to the octarepeat region has recently been shown to induce β-sheet formation in the unstructured domain [34].

Nevertheless, it has been possible to gather some structural insights into the copper-bound states of the N-terminal region of PrP using combinations of NMR, CD, electron paramagnetic resonance (EPR) techniques, and extended X-ray absorption fine structure (EXAFS) spectroscopy [35; 36]. In particular, the latter technique permits investigation of the coordination of copper in the complex with octarepeat peptides. Furthermore, it is possible to obtain an X-ray structure of a peptide HGGGW-Cu^{2+} [37]. The NMR structures [32; 33] display reasonable agreement with the backbone geometry of the crystal structure of the copper-loaded pentapeptide. It appears that β-turn structures are formed from segments encompassing GWGQ [32], and that WGQPH also forms a loop-like core structure [33]. However, the side-chain orientation of the tryptophane residue differs about 180° from the structures obtained from X-ray and NMR studies. Recent EXAFS and EPR studies proposed a three-dimensional structure of a single octarepeat peptide involving a planar coordination of copper with three nitrogen atoms and one oxygen atom [36]. Ap-

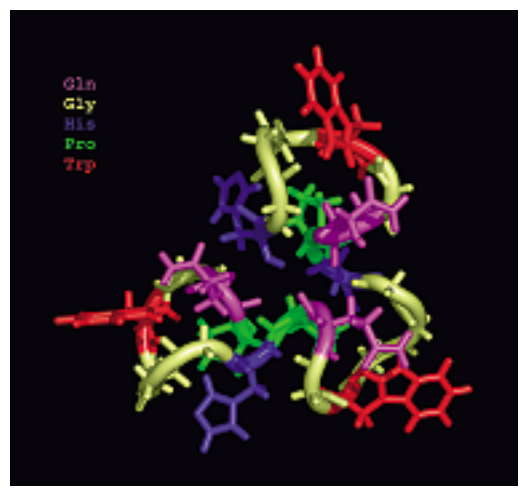

Fig. 6.11: Structure of the copper-free octarepeat residues 61–84 (PDB code 1OEI). ©: Figure by S. Schwarzinger with PyMOL, DeLano Scientific, San Francisco.

parently, a picture of the octarepeat is emerging, in which the nonglycine residues (WGQPH) form a well-structured core linked by three glycine residues (Fig. 6.11). As a result of these studies, it seems that free octarepeat and copper-loaded forms share a high degree of structural similarity. A promising route for obtaining structural insights into the copper-loaded form at high resolution was recently taken by using diamagnetic nickel ions in a ^{1}H-NMR investigation to show that the six copper ions can be bound in the flexible N-terminus of PrP [38]. In particular, this study suggests that each of His96 and His111 are involved in the binding of one copper ion, independent of each other (see also Section 6.4.2).

6.4 NMR studies on isolated structural features of PrP

6.4.1 Peptide studies

While NMR studies on full-length proteins yield a wealth of information on structure and dynamics of a protein in its native context, examining the solution behavior of smaller fragments can provide valuable insights on the behavior and structural preference of smaller parts under deviation from the native environment. This is especially interesting in the case of PrP, as this particular protein undergoes massive structural changes during the conformational transition from PrP^{C} to PrP^{Sc}, in which parts of the protein are excluded from their native environment, possibly populating structural ensembles of unfolded or at least highly dynamic species. The highly dynamic behavior of short peptides in solution might therefore provide a valuable model system for intermediates in prion conversion. Such studies, however, are usually not able to yield structures or even structural models, as there are usually no well-defined distance constraints in such systems. Nevertheless, analysis of chemical shifts and their deviation from random coil values can give information on the existence or propensity of secondary structure elements and their population, even in only partially folded proteins [3; 39]. Additionally, the existence of regular $i, i+3$ and $i, i+4$ NOE connectivity patterns can point out the existence of helices in such peptide systems even at low abundance averaged over time.

Of special interest in this regard are peptide studies on regions which are supposed to take part in the conformational conversion of the PrP. Several studies focused on the region containing the β-sheet, helix 1, and the connecting loops (residues 125–170), which has been suggested to form an initiation site during the conformational transition [8].

Contrary to the expected intrinsic tendency to form sheet-like structures, it was shown that peptides huPrP(125–170), huPrP(142–170), and huPrP(154–170) adopted mainly helical conformers in aqueous solution [40]. The strongest tendency to form helices was observed for the sequence corresponding to helix 1 (145–154). Interestingly, both β-strands did not show any tendency to adopt extended conformations. Additional peptide studies focused on helix 1 in murine [15] and human [41] PrP, and further corroborated the high intrinsic tendency of this sequence to populate helical conformers. Because of its exceptionally high helix propensity helix 1 has been proposed as an energetic barrier in the pathogenic transformation [41].

Other peptide studies on PrP focused on the unstructured amino terminal domain, for which conformational information is largely inaccessible in full-length PrP. The amino terminal sequence of bovine PrP, boPrP(1–30), was shown to populate helical conformers in solutions containing DHPC micelles, thereby simulating a membrane environment [42]. In combination with deuterium exchange data and NMR studies on magnetically aligned micelles, this study points to the insertion of a helical part of this peptide in the membrane in a stable and rigid way. The function of this sequence as a cell-penetrating peptide might play a role in the cell surface accumulation of PrP, facilitating membrane translocation and possibly pathogenesis.

6.4.2 Interaction studies

Observation of chemical shift changes in a protein upon ligand binding is a sensitive method for measuring the strength of an interaction and

for defining the protein's interaction surface. Especially useful and sensitive are, for example, heteronuclear single quantum correlation (HSQC) spectra [43]. A ^{1}H-^{15}N-HSQC experiment correlates the chemical shift of a ^{15}N-nitrogen nucleus of an NH_x group with the chemical shift of a directly attached protons. Each resonance signal in the HSQC spectrum thus represents a proton that is directly bound to a ^{15}N-nitrogen atom (H^N proton). Therefore, the spectrum contains the signals of the H^N protons and ^{15}N-nitrogens in the protein backbone. Since there is one backbone H^N per amino acid (except for proline), each HSQC signal represents one single amino acid. Because the chemical shifts of the nuclei whose resonances appear in the HSQC are sensitive to their chemical environment, any binding of a ligand molecule in the vicinity induces changes in chemical shifts (''chemical shift perturbation'') of the HSQC cross resonances of the respective amide protons and nitrogens. Therefore, one can conclude, that those amino acid residues that show changes in the chemical shifts of their resonances upon addition of a ligand are somehow affected by the ligand binding. One may further conclude, that these residues build up the ligand binding site, although this is not exactly the same statement. Other experiments to map ligand binding sites are, for example, cross-saturation experiments.

Using such methods, details for the interaction of murine PrP with the SH3 domain of the signal transduction protein Grb2 could be elucidated. The existence of the interaction itself had been known before [44]. NMR spectroscopy, however, revealed the structural and dynamical nature of the interaction site on PrP. Differences in hetNOEs, indicating a change in backbone flexibility upon ligand binding, identified the segment moPrP(101–105) as the interaction site [45]. This sequence fulfils the requirements of a classical SH3 binding motif consisting of at least two proline residues separated by exactly two residues (PxxP), and replacement of either of the two proline residues abolishes the binding. This is especially interesting in the light of the Pro102Leu mutation, a common cause for several familiar TSEs in humans [46], implicating the loss of the Grb2-modulated signal transduction pathway from PrP as a possible cause of the neuropathology of TSEs in humans.

Apart from interactions with other proteins, NMR can also reveal details about the interaction of proteins with smaller ligands. By monitoring the ^{1}H -^{15}N heteronuclear correlation spectra of ^{15}N-labeled huPrP in the absence and presence of the tricyclic aromatic molecule quinacrine, it was found that quinacrine binds to a region formed by residues Tyr225, Tyr226, and Gln227 in helix 3 of PrP [47]. Quinacrine, long known to be an anti-malarial medication, was previously shown to cure cultured cells from PrP^{Sc} infection [48]. As the carboxyterminal region of helix 3 is considered a putative binding site for protein X, quinacrine might interfere with the PrP–protein X interaction, thereby preventing the conformational transition of PrP to its pathogenic isoform [47].

Further interaction studies on PrP have concentrated on copper binding to PrP, which has been proposed to play a significant role in maintaining and regulating synaptic copper concentrations [49]. In addition to the known copper-binding properties of the octarepeat region (see Section 6.3), NMR spectroscopy revealed interactions of the sequences huPrP(106–113) and huPrP(106–126) with copper ions. Copper binding is modulated by the residues Lys106, Lys110, and His111 [50]. For the binding of manganese ions to huPrP(106–126), similar effects were observed [51]. Interestingly, ion coordination and peptide conformation differ for Cu^{2+} and Mn^{2+} ions, which might have implications for the mechanism of neurotoxicity this peptide exhibits in the presence of some bivalent metal ions.

6.4.3 Hydrogen exchange studies of protein dynamics

NMR experiments that monitor hydrogen exchange of proteins form, by some means, a middle ground between structural and dynamical information. The key principle is based on the loss of signal intensity occurring after exchange of protons with deuterons in proteins

solvated in heavy water (D_2O). Most experiments focus on the amide protons of the protein backbone. Apart from environmental conditions, such as pH and temperature, hydrogen exchange is predominantly governed by the solvent accessibility of the relevant protons. Therefore, it is a method for the direct detection of solvent accessibility, as well as an indirect method to measure backbone flexibility; backbone motions can render amide protons, which seem to be protected from solvent interaction in the average structure accessible to solvent. Additionally, hydrogen bonding has a significant influence on hydrogen exchange, lowering the observed exchange rates.

Not surprisingly, hydrogen exchange experiments performed on Syrian hamster PrP (shPrP) showed most protected residues located within the regular secondary structure elements of the folded carboxyterminal domain. The strongest protection from hydrogen exchange is observed for helices 2 and 3, whereas helix 1 and both strands of the β-sheet exhibit only intermediate protection, indicating elevated dynamic behavior of those regions [52]. The carboxyterminal ends of helices 2 and 3, however, exhibit lower protection factors than the remaining parts of those helices, which points to the existence of an equilibrium between helical and unfolded states in these regions. Similar observations were reported in experiments on the huPrP [16]. However, it should be pointed out that the protection factors observed for the PrP are comparatively small compared to other well-structured proteins. This may indicate a certain degree of structural breathing, even in the core of the protein. A recent crystallographic study revealed the existence of water molecules buried inside the folded core [53]. The authors could also establish a possible role of these structural water molecules for the stability of the protein.

Furthermore, hydrogen exchange studies are suited to identify regions of the hydrogen bonded backbone which remain stable until the protein is fully unfolded. Kinetic analysis identifies those residues whose protection factors are characteristic for exchange from the unfolded form, rather than from the folded state or from unfolding intermediates. By this approach, regions of the protein which remain folded during the whole unfolding process can be identified. Application of this method to the PrP revealed a core of hyperstable residues, which basically coincide with the core residues of the natively folded protein [54]. As this indicates the persistence of the basic fold throughout the whole unfolding process, the protein has necessarily to go through a nearly completely unfolded state in order to adopt an alternative, β-rich conformation.

Recent methodical advancements [55] allow the investigation of hydrogen-exchange rates in the fibrillar state. The method is based on the very slow exchange rates of protein amide protons in mixtures of organic solvents, such as DMSO, with D_2O. Fibril preparations are exposed to D_2O and are subsequently transferred to a DMSO/D_2O mixture to quench the exchange process and to dissolve the fibrils into their monomers. The latter are then investigated by solution NMR studies to determine which amide protons had exchanged during D_2O exposure. Application of this method to fibrils of the amyloidogenic peptide huPrP(106–126) yielded interesting information on possible conformational behavior of the peptide in its fibrillar state [56]. Hydrogen exchange data under these conditions support models derived from molecular dynamics simulation, depicting the fibrillar structure as a stack of four stranded parallel sheets, shown by the existence of single-exponential exchange kinetics in the central part of the peptide.

6.5 High pressure NMR

Whereas the abovementioned methods mostly focused on the native state of PrP, high pressure NMR presents an approach to the characterization of alternative conformations. Perturbing the native state by application of high pressures allows observation of rare conformers, which become stable under such thermodynamic conditions [57]. Under high pressure, the solvated protein can principally react in two ways: (i) reduction of effective volume by general compression of the structure (indicated by linear

change of chemical shifts with pressure increase), or by reduction of effective volume by shifting the equilibrium between at least two different conformations (indicated by nonlinear changes in spectral parameters with increasing pressure).

High pressure studies on the PrP revealed the existence of a metastable, only slightly populated alternative conformer of PrP, which has been hypothesized to be identical to the postulated conversion intermediate PrP^{-} [58]. This intermediate is characterized by transient helix formation in the amino terminal region and within the hydrophobic cluster. Anomalous, nonlinear shift deviations could be observed for the strand 1–helix 1 region, as well as for the loops between helix 1 and strand 2, and the loop between helices 2 and 3. Such alterations can be indicative of hinge motions altering the global structure. Interestingly, regions of conformational instability coincide with regions in which most pathogenic mutations of huPrP cluster together. In a more recent study high-pressure NMR measurements were combined with NMR relaxation measurements [59]. This study reveals regions of complex conformational mobility that cluster in the short antiparallel β-sheet and parts of helices 2 and 3. They are in agreement with the earlier observations [30] that suggest a conformational exchange in strand 1. The same study indicates that the helix 2–helix 3 interface, where many pathogenic mutations cluster, undergoes slow motions, which is somewhat in contrast to the deuterium experiments reported above.

6.6 Structural studies on PrP^{Sc}

In contrast to the soluble and crystallizable PrP^{C}, PrP^{Sc} is not directly accessible for structure determination by NMR or X-ray. The insolubility and strong tendency to form fibrils and rather amorphous aggregates renders this isoform inaccessible to classical methods of structure determination. For this reason, no high-resolution structure of PrP^{Sc} is available up to now.

It is, however, possible to gain insight into several structural features of PrP^{Sc} by various biophysical methods. Solid-state NMR is able to retrieve information on the structural behavior of prion peptide aggregates. While it is not yet possible to obtain high-resolution structures from such experiments, they nevertheless can yield information of secondary structure distributions in the aggregated conformation. Significant differences in secondary structure distribution between the fibrillar and the randomly aggregated, amorphous form of moPrP(89–143) were found for several PrP variants. Especially the Pro102Leu variant exerted significant long-range effects on the conformation of the peptide, showing a strong shift of the conformational distribution towards the mostly extended structures. Similarly, introduction of several alanine to valine exchanges in the palindromic AGAAAAGA-region of shPrP, shifted the conformational distribution of PrP from helical to extended [60]. Interestingly, the mere presence of extended conformers seems not to be sufficient to stimulate disease in animal models. This indicates the necessity of very specific, highly defined conformations for the interaction with PrP^{C} and the development of dis-

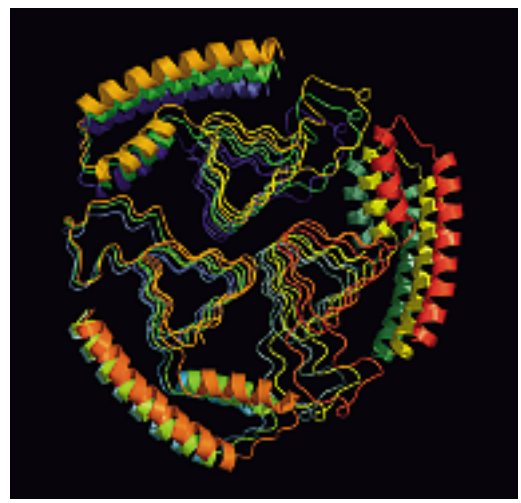

Fig. 6.12: Schematic model of the proposed β-helical conformation of PrP^{Sc}. PrP molecules are arranged in trimeric discs that can staple thereby forming fibrils. The model was constructed as described [64]. Coordinates for Figure 6.12 were kindly provided by M. Stork, LMU Munich. ©: Figure by S. Schwarzinger with PyMOL, DeLano Scientific, San Francisco.

ease. Further evidence for high conformational flexibility of the fibrillar form of the huPrP(109–122) region were concluded from the contents of secondary structure elements in aggregates of this peptide prepared from different solution conditions [61].

A global picture of PrP^{Sc}, albeit with low resolution was obtained using negative stain electron microscopy on two-dimensional crystals of PrP^{Sc} [62]. The method yielded rough structures with a resolution of 0.7 nm, which subsequently could be fitted to a right-handed β-helical model structure based on the structure of the *Methanosarcina thermophila* carbonic anhydrase. Interestingly, the models show helices 2 and 3, which are linked by the intramolecular disulfide bond, retaining their helical conformation. In the remaining part of the protein, consisting of the unstructured amino terminal domain, the β-sheet and helix 1 are incorporated into the β-helix. This underscores the abovementioned importance of the β-strand 1–helix 1–β-strand 2 region for the conformational transition, as this region has to undergo a complete structural rearrangement during conversion to the pathological isoform. Further evidence for the arrangement of such β-helical subunits into a trimeric superstructure could subsequently be obtained by low-resolution fiber diffraction, electron microscopy (EM), and atomic force microscopy (AFM) [63], as well as from molecular modeling studies, as shown in Fig. 6.12 [64].

References

[1] Pervushin K, Riek R, Wider G, et al. Attenuated T2 relaxation by mutual cancellation of dipole–dipole coupling and chemical shift anisotropy indicates an avenue to NMR structures of very large biological macromolecules in solution. Proc Natl Acad Sci USA 1997; 94:12366–12371.

[2] Wüthrich, K. NMR of proteins and nucleic acids. John Wiley & Sons, New York, 1986.

[3] Wishart DS, Sykes BD, Richards FM. The chemical shift index: a fast and simple method for the assignment of protein secondary structure through NMR spectroscopy. Biochemistry 1992; 31:1647–1651.

[4] Brown DR, Qin K, Herms JW, et al. The cellular prion protein binds copper in vivo. Nature 1997; 390:684–687.

[5] Glockshuber R, Hornemann S, Riek R, et al. Three-dimensional NMR structure of a self-folding domain of the prion protein PrP(121–231) [letter; comment]. Trends Biochem Sci 1997; 22:241–242.

[6] Hornemann S, Korth C, Oesch B, et al. Recombinant full-length murine prion protein, mPrP(23–231): purification and spectroscopic characterization. FEBS Lett 1997; 413:277–281.

[7] Zahn R, von Schroetter C, Wuthrich K. Human prion proteins expressed in *Escherichia coli* and purified by high-affinity column refolding. FEBS Lett 1997; 417:400–404.

[8] Riek R, Hornemann S, Wider G, et al. NMR structure of the mouse prion protein domain PrP(121–321). Nature 1996; 382:180–182.

[9] James TL, Liu H, Ulyanov NB, et al. Solution structure of a 142-residue recombinant prion protein corresponding to the infectious fragment of the scrapie isoform. Proc Natl Acad Sci USA 1997; 94:10086–10091.

[10] Hornemann S, Schorn C, Wuthrich K. NMR structure of the bovine prion protein isolated from healthy calf brains. EMBO Rep 2004; 5:1159–1164.

[11] Calzolai L and Zahn R. Influence of pH on NMR structure and stability of the human prion protein globular domain. J Biol Chem 2003; 278:35592–35596.

[12] Glockshuber R, Hornemann S, Billeter M, et al. Prion protein structural features indicate possible relations to signal peptidases [published erratum appears in FEBS Lett 1998 Jul 10; 431(1):130]. FEBS Lett 1998; 426:291–296.

[13] Kaneko K, Zulianello L, Scott M, et al. Evidence for protein X binding to a discontinuous epitope on the cellular prion protein during scrapie prion propagation. Proc Natl Acad Sci USA 1997; 94:10069–10074.

[14] Korth C, Stierli B, Streit P, et al. Prion (PrP^{Sc})-specific epitope defined by a monoclonal antibody. Nature 1997; 390:74–77.

[15] Liu A, Riek R, Zahn R, et al. Peptides and proteins in neurodegenerative disease: helix propensity of a polypeptide containing helix 1 of the mouse prion protein studied by NMR and CD spectroscopy. Biopolymers 1999; 51:145–152.

[16] Zahn R, Liu A, Luhrs T, et al. NMR solution structure of the human prion protein. Proc Natl Acad Sci USA 2000; 97:145–150.

[17] Lopez Garcia F, Zahn R, Riek R, et al. NMR structure of the bovine prion protein. Proc Natl Acad Sci USA 2000; 97:8334–8339.
[18] Lysek DA, Schorn C, Nivon LG, et al. Prion protein NMR structures of cats, dogs, pigs, and sheep. Proc Natl Acad Sci USA 2005; 102:640–645.
[19] Gossert AD, Bonjour S, Lysek DA, et al. Prion protein NMR structures of elk and of mouse/elk hybrids. Proc Natl Acad Sci USA 2005; 102:646–650.
[20] Calzolai L, Lysek DA, Perez DR, et al. Prion protein NMR structures of chickens, turtles, and frogs. Proc Natl Acad Sci USA 2005; 102:651–655.
[21] Haire LF, Whyte SM, Vasisht N, et al. The crystal structure of the globular domain of sheep prion protein. J Mol Biol 2004; 336:1175–1183.
[22] Knaus KJ, Morillas M, Swietnicki W, et al. Crystal structure of the human prion protein reveals a mechanism for oligomerization. Nat Struct Biol 2001; 8:770–774.
[23] Billeter M, Riek R, Wider G, et al. Prion protein NMR structure and species barrier for prion diseases. Proc Natl Acad Sci USA 1997; 94:7281–7285.
[24] Liemann S and Glockshuber R. Influence of amino acid substitutions related to inherited human prion diseases on the thermodynamic stability of the cellular prion protein. Biochemistry 1999; 38:3258–3267.
[25] Zhang Y, Swietnicki W, Zagorski MG, et al. Solution structure of the E200K variant of human prion protein. Implications for the mechanism of pathogenesis in familial prion diseases. J Biol Chem 2000; 275:33650–33654.
[26] Hosszu LL, Jackson GS, Trevitt CR, et al. The residue 129 polymorphism in human prion protein does not confer susceptibility to Creutzfeldt–Jakob disease by altering the structure or global stability of PrP^{C}. J Biol Chem 2004; 279:28515–28521.
[27] Donne DG, Viles JH, Groth D, et al. Structure of the recombinant full-length hamster prion protein PrP(29–231): the N terminus is highly flexible. Proc Natl Acad Sci USA 1997; 94:13452–13457.
[28] Riek R, Hornemann S, Wider G, et al. NMR characterization of the full-length recombinant murine prion protein, mPrP(23–231). FEBS Lett 1997; 413:282–288.
[29] Zahn R. Prion propagation and molecular chaperones. Q Rev Biophys 1999; 32:309–370.
[30] Viles JH, Donne D, Kroon G, et al. Local structural plasticity of the prion protein. Analysis of NMR relaxation dynamics. Biochemistry 2001; 40:2743–2753.
[31] Jackson GS, Murray I, Hosszu LL, et al. Location and properties of metal-binding sites on the human prion protein. Proc Natl Acad Sci USA 2001; 98:8531–8535.
[32] Zahn R. The octapeptide repeats in mammalian prion protein constitute a pH-dependent folding and aggregation site. J Mol Biol 2003; 334:477–488.
[33] Renner C, Fiori S, Fiorino F, et al. Micellar environments induce structuring of the N-terminal tail of the prion protein. Biopolymers 2004; 73:421–433.
[34] Jones CE, Abdelraheim SR, Brown DR, et al. Preferential Cu^{2+} coordination by His96 and His111 induces beta-sheet formation in the unstructured amyloidogenic region of the prion protein. J Biol Chem 2004; 279:32018–32027.
[35] Viles JH, Cohen FE, Prusiner SB, et al. Copper binding to the prion protein: structural implications of four identical cooperative binding sites. Proc Natl Acad Sci USA 1999; 96:2042–2047.
[36] Mentler M, Weiss A, Grantner K, et al. A new method to determine the structure of the metal environment in metalloproteins: investigation of the prion protein octapeptide repeat $Cu^{(2+)}$ complex. Eur Biophys J 2005; 34:97–112.
[37] Burns CS, Aronoff-Spencer E, Legname G, et al. Copper coordination in the full-length, recombinant prion protein. Biochemistry 2003; 42:6794–6803.
[38] Jones CE, Klewpatinond M, Abdelraheim SR, et al. Probing copper2+ binding to the prion protein using diamagnetic $nickel^{2+}$ and 1H NMR: the unstructured N terminus facilitates the coordination of six $copper^{2+}$ ions at physiological concentrations. J Mol Biol 2005; 346:1393–1407.
[39] Schwarzinger S, Kroon GJ, Foss TR, et al. Sequence-dependent correction of random coil NMR chemical shifts. J Am Chem Soc 2001; 123:2970–2978.
[40] Sharman GJ, Kenward N, Williams HE, et al. Prion protein fragments spanning helix 1 and both strands of beta sheet (residues 125–170) show evidence for predominantly helical propensity by CD and NMR. Fold Des 1998; 3:313–320.
[41] Ziegler J, Sticht H, Marx UC, et al. CD and NMR studies of prion protein (PrP) helix 1. Novel implications for its role in the PrP^{C}–PrP^{Sc} conversion process. J Biol Chem 2003; 278:50175–50181.
[42] Biverstahl H, Andersson A, Graslund A, et al. NMR solution structure and membrane interac-

tion of the N-terminal sequence (1–30) of the bovine prion protein. Biochemistry 2004; 43:14940–14947.

[43] Görlach M, Wittekind M, Beckman RA, et al. Interaction of the RNA-binding domain of the hnRNP C proteins with RNA. Embo J 1992; 11:3289–3295.

[44] Spielhaupter C and Schatzl H.M. PrP^{C} directly interacts with proteins involved in signaling pathways. J Biol Chem 2001; 276:44604–44612.

[45] Lysek DA and Wuthrich K. Prion protein interaction with the C-terminal SH3 domain of Grb2 studied using NMR and optical spectroscopy. Biochemistry 2004; 43:10393–10399.

[46] Telling GC, Haga T, Torchia M, et al. Interactions between wild-type and mutant prion proteins modulate neurodegeneration in transgenic mice. Genes Dev 1996; 10:1736–1750.

[47] Vogtherr M, Grimme S, Elshorst B, et al. Antimalarial drug quinacrine binds to C-terminal helix of cellular prion protein. J Med Chem 2003; 46:3563–3564.

[48] Doh-Ura K, Iwaki T, Caughey B. Lysosomotropic agents and cysteine protease inhibitors inhibit scrapie-associated prion protein accumulation. J Virol 2000; 74:4894–4897.

[49] Brown DR and Sassoon J. Copper-dependent functions for the prion protein. Mol Biotechnol 2002; 22:165–178.

[50] Belosi B, Gagelli R, Guerrini R, et al. Copper binding to the neurotoxic peptide PrP106–126: thermodynamic and structural studies. Chembiochem 2004; 5:349–359.

[51] Gaggelli E, Bernardi F, Molteni E, et al. Interaction of the human prion PrP(106–126) sequence with copper(II), manganese(II), and zinc(II): NMR and EPR studies. J Am Chem Soc 2005; 127:996–1006.

[52] Liu H, Farr-Jones S, Ulyanov B, et al. Solution structure of Syrian hamster prion protein rPrP(90–231). Biochemistry 1999; 38:5362–5377.

[53] De Simone A, Dodson GG, Verma CS, et al. Prion and water: tight and dynamical hydration sites have a key role in structural stability. Proc Natl Acad Sci USA 2005; 102:7535–7540.

[54] Hosszu LL, Baxter NJ, Jackson GS, et al. Structural mobility of the human prion protein probed by backbone hydrogen exchange. Nat Struct Biol 1999; 6:740–743.

[55] Ippel JH, Olofsson A, Schleucher J, et al. Probing solvent accessibility of amyloid fibrils by solution NMR spectroscopy. Proc Natl Acad Sci USA 2002; 99:8648–8653.

[56] Kuwata K, Matumoto T, Cheng H, et al. NMR-detected hydrogen exchange and molecular dynamics simulations provide structural insight into fibril formation of prion protein fragment 106–126. Proc Natl Acad Sci USA 2003; 100:14790–14795.

[57] Akasaka K. Highly fluctuating protein structures revealed by variable-pressure nuclear magnetic resonance. Biochemistry 2003; 42:10875–10885.

[58] Kuwata K, Li H, Yamada H, et al. Locally disordered conformer of the hamster prion protein: a crucial intermediate to PrP^{Sc}? Biochemistry 2002; 41:12277–12283.

[59] Kuwata K, Kamatari YO, Akasaka K, et al. Slow conformational dynamics in the hamster prion protein. Biochemistry 2004; 43:4439–4446.

[60] Laws DD, Bitter HM, Liu K, et al. Solid-state NMR studies of the secondary structure of a mutant prion protein fragment of 55 residues that induces neurodegeneration. Proc Natl Acad Sci USA 2001; 98:11686–11690.

[61] Heller J, Kolbert AC, Larsen R, et al. Solid-state NMR studies of the prion protein H1 fragment. Protein Sci 1996; 5:1655–1661.

[62] Wille H, Michelitsch MD, Guenebaut V, et al. Structural studies of the scrapie prion protein by electron crystallography. Proc Natl Acad Sci USA 2002; 99:3563–3568.

[63] Govaerts C, Wille H, Prusiner SB, et al. Evidence for assembly of prions with left-handed beta-helices into trimers. Proc Natl Acad Sci USA 2004; 101:8342–8347.

[64] Stork M, Giese A, Kretzschmar HA, et al. Molecular dynamics simulations indicate a possible role of parallel beta-helices in seeded aggregation of poly-Gln. Biophys J 2005; 88:2442–2451.